SURVEYING & SPATIAL SCIENCES CONFERENCE 2013

Proceedings of the SURVEYING & SPATIAL SCIENCES CONFERENCE 2013
17 - 19 April 2013 Canberra Australia

EFFECTS OF SPATIAL RESOLUTION ON MEASUREMENT OF LANDSCAPE FUNCTION USING THE LANDSCAPE LEAKINESS CALCULATOR

by
Ernest Dunwoody, Armando Apan and Xiaoye Liu
Faculty of Engineering and Surveying &
Australian Center for Sustainable Catchments,
University of Southern Queensland,
Toowoomba, QLD 4350 Australia

ABSTRACT

This study investigated the effect of changes in the scale of imagery on landscape elements and in turn on calculating the loss of resources in a rangeland catchment. The CSIRO Leakiness Calculator was used as the analytic tool to measure the leakiness of the experimental catchment under a variety of scenarios.

The approach was to use concurrent images of the same catchment area captured at different native resolutions and to upscale the high resolution image to match the lower resolution images to see the effect on calculated catchment leakiness. Two indices, the Stress-related Vegetation Index (STVI) and the Redness Index (RI) were used to measure land cover. The experimental catchment covered about 6,000 ha south-west of Charters Towers in North Queensland.

The two cover indices produced markedly different cover and leakiness results and these results varied with native image scale. The upscaled images also yielded different cover and leakiness results which did not coincide with comparable native scale image analyses.

The causes of the lack of agreement between the results were investigated using semivariance analysis techniques. The calculated leakiness of the native scale images showed no clearly defined relationship with the resolution-dependent amount of cover or the sill semivariance but it was strongly correlated with the negative power of the image resolution. The calculated leakiness of the upscaled image had a strong negative power correlation with the resolution-dependent amount of cover, image resolution and sill semivariance.

The findings highlight the importance of carefully considering all input variables including image preprocessing, type of cover index and resolution of the image when comparing the leakiness of different catchments using the Leakiness Calculator. These results indicate that it may be not possible to make meaningful comparisons of landscape leakiness of the same area between images of different scales or from different sensors.

KEYWORDS

catchment monitoring, landscape condition, resource loss, leakiness, scaling

1 INTRODUCTION

There is a growing need to assess the ecological condition of rangeland catchments due to increased grazing pressure, climate change impacts and downstream water quality concerns. A range of archival and on-demand imagery sources spanning different time periods, collected at different resolutions and by different sensors is available. The large areas of rangeland involved necessitate multi-scene and multi-temporal comparisons and the production of aggregated data to provide overview assessments. To date there has been no reported evaluation of the comparability of ecosystem condition monitoring from images at different scales and from different sensors..

The role of landscape elements is fundamental to the resource conserving nature of resource limited landscapes. Scale strongly affects the recognition of these landscape features in imagery (De Jong et al., 2011) however its effect on calculating the loss of resources (leakiness) from

imagery has not been addressed to date. The CSIRO Leakiness Calculator (Ludwig et al., 2006) is software that uses a Digital Elevation Model, a catchment analysis mask and a landscape cover image to calculate the leakiness of a catchment. It was the primary analytical tool used in this study.

The study objectives were to find out:

i. What is the relative leakiness response of the same temporal scene at different native resolutions?
ii. How does leakiness respond to scene up-scaling?
iii. What is the relationship between native scene and up-scaled scene leakiness at the same resolution?
iv. What causes the response in iii above?

2 ECOSYSTEM FUNCTION

2.1 Landscape Function Measurement

Landscape Function Analysis (LFA) began as a manual field based method of recording and analyzing features of the landscape that could be relied upon to yield consistent indicators of ecosystem condition (Tongway et al., 2004). New techniques using satellite imagery to monitor surrogates of ecosystem function are replacing field based measurements (Bastin et al., 2002; Scarth et al., 2008; Bastin et al., 2012; Schmidt et al., in prep). These include measurements of the abundance, condition and relative position of landscape features as well as their changes over time.

The banded vegetation patterns that are a common theme in Australian rangelands are due to topographic and landscape hydrological processes (Tongway et al., 1990). A Trigger, Transfer, Reserve, Pulse (TTRP) model was shown to explain how the natural features of wind, water and landscape elements combined to conserve and utilize resources (Ludwig et al., 1997). These process are three dimensional and operate in both banded and non-banded landscapes and at small and large scales (Wilcox et al., 2003). They indicate the type of landscape features that can be measured to assess temporal changes in landscape function.

Spatial resolution of an image determines how landscape features are recorded at the pixel level through setting the sampling interval and the support base (Atkinson 2004) for the image. Ecosystem function also varies with the size of the landscape feature (Ludwig et al., 2000) and this “double-scale effect” compounds the interpretation of landscape function from imagery. Most imagery based LFA measurements have been based on Landsat images with pixel sizes ranging from 25 to 80m (Bastin et al., 2008). To be able to analyse changes in rangeland condition over extended time periods and geographical extents it is necessary to use different types of imagery with different resolutions. This requires that we know the effect of image resolution on measurement of landscape function. Analysis of the pattern of the Perpendicular Distance cover index of the red band over the green band (PDr/g) (Pickup et al., 1993) for sites at different distances from livestock watering points showed a strong correlation with land condition measurements. A similar pattern of land condition was also observed at the catchment scale (Ludwig et al., 2004). These studies showed a consistent correlation between quantity and quality of vegetation patches and land condition at both coarse and fine scales. This suggested the measurement of intactness of ground cover and greenness of patches as surrogates for the resource conserving condition of the landscape. The use of satellite imagery to record these attributes over large areas offers the opportunity for increased use of LFA in land management and policy setting (Ludwig et al., 2004).

2.2 Leakiness Calculation

A sequence of automated leakiness calculation procedures was developed by Ludwig et al consisting of the Directional Leakiness Index (2002), the Cover Based Directional leakiness Index (2006) and the Leakiness Calculator (LC) (2007a). The LC incorporates both elevation and cover data in a distributed flow calculation based on the T Hydro approach (Ostendorf et al., 1993) to allow accumulation and flow to and from all neighbouring pixels. The procedure calculates the total leakiness exiting from the pour point of a catchment by an equation in the following form:

where ,

in which c = pixel cover index value (%), and

b = -0.065, the steepness of a graph of the decline in soil loss with increasing cover (Ludwig et al., 2007a).

This relationship was found to provide consistent and verifiable results when historical Landsat imagery of a rangeland site with a known grazing management history was analysed (Bastin et al., 2002). Testing of the Leakiness Calculator at different scales in rangeland in the Fanning River catchment in the dry tropics area of North Queensland (Bastin et al., 2008) found that:

i. there was a clear inverse relationship (as expected) between leakiness and cover when tested at a fine scale ($5m^2$),
ii. the relationship between leakiness values derived from the Landsat based Ground Cover Index ($25m^2$) (Scarth et al., 2008) of catchment condition was consistent, and
iii. there was no consistent relationship between leakiness and PATCHKEY data (Corfield et al., 2006) collected from 100-$200m^2$ patches.

The Calculator produces a series of analyses for each catchment. These include the Average Cover (%), Calculated Leakiness (L Calc) and the Leakiness Index (LI). The average cover and calculated leakiness were the two measures used in this analysis. The Leakiness Index was not used because it is a normalized value derived by dividing the calculated leakiness value by a user selected variable maximum leakiness setting, sufficient to yield an Index ranging from 0 – 1. This is useful for comparing the leakiness performance of catchments but not for analysing the behaviour of cover, leakiness and variance between different cover indices and at different scales.

2.3 Scaling Effects

There are two types of spatial scale in images, scale of measurement and scale of variation (Atkinson et al., 2000). As well, images also exist within a temporal scale as reflected by their date of capture. Spatial data are the result of sampling at a particular measurement scale (interval and support) and contain within them the spatial variation associated with that scale of measurement. Leakiness measurement relies on the type and location of cover features in a catchment. The scale determines the features and their spatial variation. These change with change in resolution, either through expression or regularisation due to the inherent autocorrelation within an image. Measuring the amount of autocorrelation in a scene provides a measure of the spatial variation which may be able to be used to measure how the leakiness of a catchment changes with change in resolution.

Change in spatial pattern affects loss or retention of features through regularisation. Turner et al., (1989) showed that landscape features that were clumped were retained when resolution was decreased while features that were dispersed were rapidly lost. Wu et al., (2002) found that different types of landscape metrics exhibited different types of responses when regularised. Their response to changes in scale were either; a) predictable (simple equations), b) stair-case like (less predictable), or c) erratic (no consistent scaling relationship). They suggested the use of metric scalograms to quantify spatial heterogeneity rather than single scale measures. Multiscale analysis was also shown to be needed to adequately characterise the diversity of features in a landscape (Wu 2004). In studies of bare-ground patches in semi-arid ecosystems Karl et al (2010) found the segmentation level whose regression predictions had a spatial dependence closest to the spatial organisation of the field samples showed the highest predicted-to-observed correlation. A range of “best” analysis scales may exist depending on the attributes being measured along with a need for methods to identify scales that perform best for specific analysis purposes.

Aggregation methods used in up-scaling images to coarser resolutions change the spatial characteristics of the image. The amount of change depends on whether the aggregation is

coarser of finer than the autocorrelation range of the parent image (Bian et al., 1999). Spatial variability and spatial structure are both able to be quantified from the semi-variance and the variogram model for a scene (Garrigues et al., 2008). Collins et al., (1999) showed that the regularised variogram provided an estimate of the resolution dependent variance and that this was independent of the spatial structure of the underlying scene.

Bradshaw et al., (2000) found that both pattern and process play an important role in determining the scale at which to monitor ecosystems. They suggested that spatial and temporal scales of the landscape features and the ecological processes be considered when selecting the spectral, spatial and temporal resolution of imagery for landscape monitoring programs. Ludwig et al., (2000) also developed rules and equations for scaling functions to integrate scale dependent landscape patterns with the ecological processes associated with them. This approach integrates the interdependency of measurement scale with ecological scale. The observation scale must allow detection of the ecologically significant landscape features from which the scaling relationships can then predict ecological behaviour. Ludwig et al., (2000) illustrated this by a rule for landscape patches, namely: "***The concentration of resources (per unit area) becomes increasingly greater as patch size increases***". They also suggested the existence of a landscape patch rule for runoff. Further work established the importance of patch configuration on resource loss (Ludwig et al., 2007b).

A primary tool for calculating rangeland condition and resource loss is the CSIRO Leakiness Calculator. The reasonableness of its predictions using ground cover data at 25m to 80m has been verified by a number of studies (Pickup et al., 1993; Bastin et al., 2008). Before this approach can be used more widely it is desirable to know how image scale affects leakiness measurements. The following section outlines the methods used to address the effect of image scale on leakiness in this study.

3 METHODOLOGY

This analysis used two measures of ground cover, the Stress related Vegetation Index (STVI) and the Redness Index (RI) to explore the comparability of catchment leakiness from concurrent images at different resolutions of the same catchment. The STVI was equivalent to STVI-4 (Thenkabail et al., 1994) reported by Jafari et al., (2007) to produce a high correlation with perennial plants and total vegetation in South Australian semi-arid rangelands. The advantage of the STVI over the NDVI is that it is reported to highlight vegetation cover in situations of moisture stress while reducing the effect of soil background reflectance. The RI (Bannari et al., 1995) was used as a general cover index for chlorophyll rich vegetation. The RI yielded a higher cover and a lower leakiness values than the STVI (Fig 4-1).

Previous leakiness studies (Pickup et al., 2000; Bastin et al., 2008) have used perpendicular vegetation indices, in particular the PD_{54} index (Pickup et al., 1993). Jafari et al., (2007) showed that the STVI-4 index performed marginally better than the PD_{54} index at their study site. The Queensland general Ground Cover Index (Scarth et al., 2006) has also been used in catchment leakiness assessments (Bastin et al., 2008). Its use was not included in this study because of the absence of confirmed procedures for calculating it from SPOT and MODIS imagery.

The overall approach was to compare the resource leakiness of an experimental catchment using original imagery at three scales that was captured at close to the same time, to upscale the higher resolution imagery to match the lower resolution imagery and to compare the calculated leakiness (L Calc) values between the native resolution imagery and the up-scaled imagery. A sub-catchment in the Selheim River basin 20 km south-west of Charters Towers, Queensland was identified as meeting the key project selection criteria of grazing land with minimal tree clearing, available DEMs, concurrent imagery from SPOT, Landsat TM5 and MODIS satellites that was cloud free and that contained Statewide Landcover and Trees Study (SLATS) reference sites (Figure 3-1).

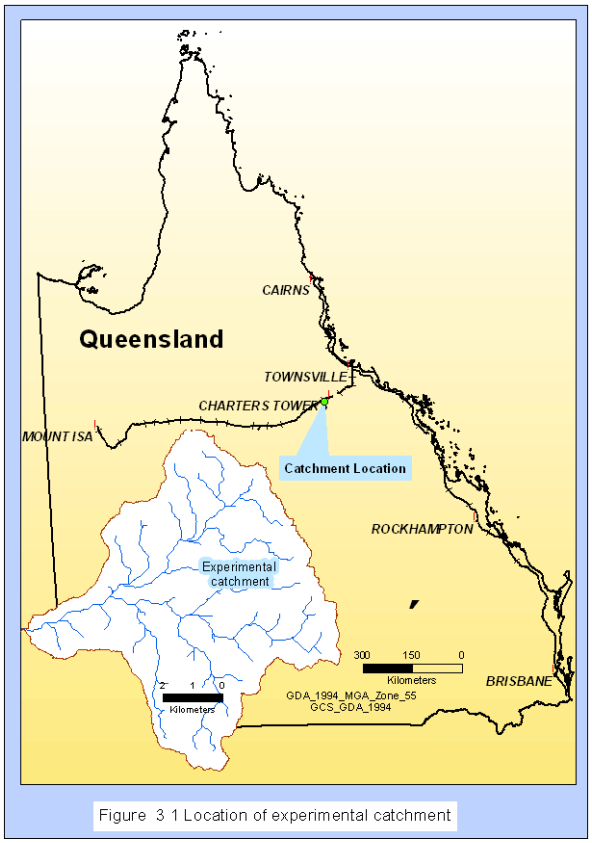

Figure 3 1 Location of experimental catchment

An overview of the processing steps is shown in Figure 3-2. The Leakiness Calculator software was used to measure the resource loss or leakiness of the experimental catchment at different spatial resolutions (Ludwig et al., 2007a). The DEM, Analysis Mask and Coverage files for use in the Leakiness Calculator were formatted according to the requirements specified by CSIRO (2007) using ERDAS Imagine, SAGA (System for Automated Geoscientific Analysis), ArcHydro and ArcGIS software. Up-scaling of the 5m DEM and 10m SPOT image was done by cubic convolution using Arc GIS. Coverage calculation was done after up-scaling. The key user controlled variables in the Leakiness Calculator are the type of ground cover measurement, grass type and the Lmax setting.

The Stress related Vegetation Index (STVI) (Jafari et al., 2007) and the Redness Index (Bannari et al., 1995) were used to estimate the amount of vegetative ground cover in the catchment. Foliage Projective Cover was not masked out of the imagery in making the ground cover estimations. “Tall tussock” was used as the grass type and Lmax was adjusted so that the Leakiness Index (LI) was close to unity for the lowest coverage in each set of analyses. This setting did not affect the total calculated leakiness (L Calc). The amount of cover (%) and calculated leakiness (Lcalc) were the key results from the Leakiness Calculator used in this study.

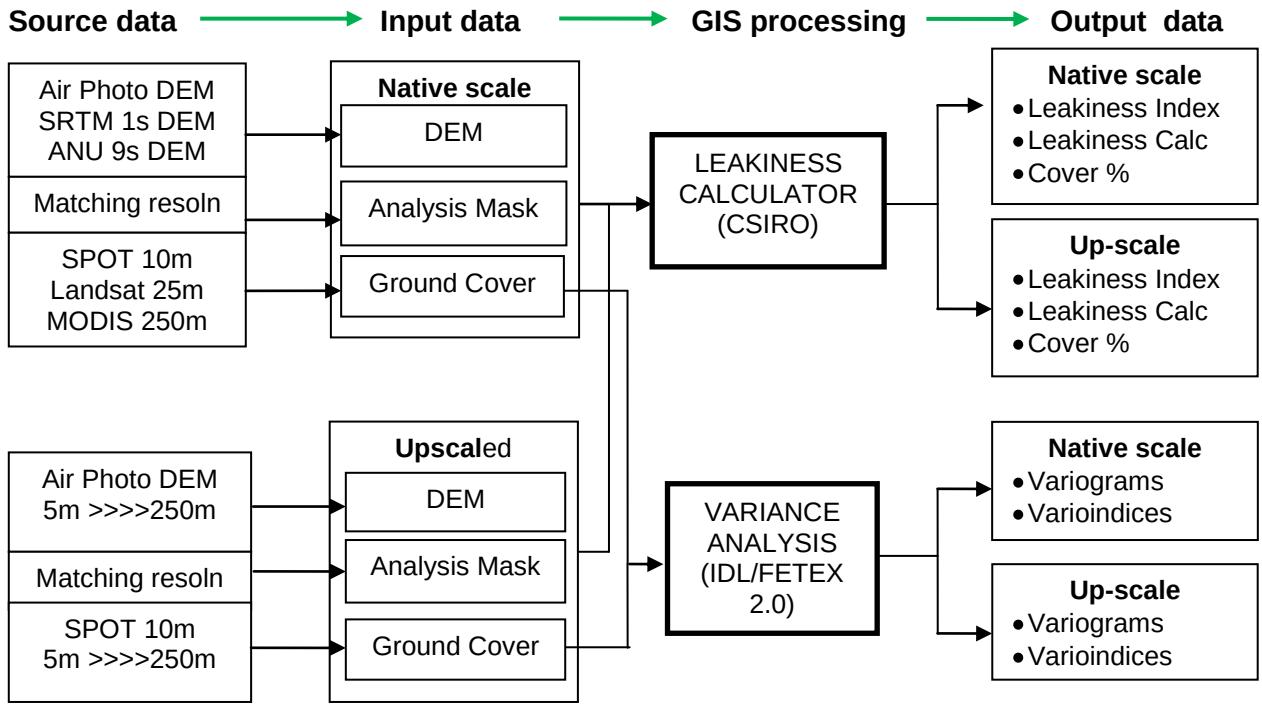

Figure 3-2 Processing procedure for Leakiness scale analysis

The spatial variance of the DEM and Coverage files used for the Leakiness Calculations were analysed using the Fetex2 IDL extension software under license from the Universidad Politecnica de Valencia, Spain (UPV) (Ruiz et al., 2011). Variograms, UPV indices (Balaguer et al., 2010) and custom variogram indices were generated and analysed statistically for explanatory relationships using SPSS and Matlab software as shown in Figure 3-3.

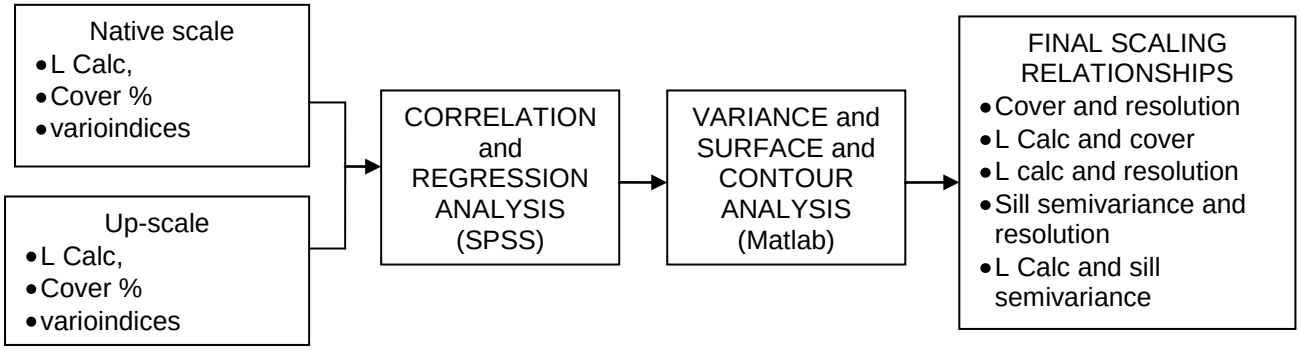

Figure 3-3 Statistical analysis and relationship development methodology

4 RESULTS

4.1 Leakiness

The leakiness of the experimental catchment is different for different measures of ground cover and these respond differently to different native image resolutions. Figure 4-1 shows the relationship between the 2 measures of ground cover, STVI and RI and the leakiness calculated from them.

The leakiness based on STVI cover is higher at higher resolutions (10 and 25m) and lower at lower resolutions (250m). When compared to the amount of STVI cover, the leakiness at 25m decreases along with a decrease in cover from the 10m values and continues to decrease at 250m, however the amount of cover increases at 250m. A different pattern occurred when leakiness was calculated from RI cover. The leakiness at 25m decreased from 10m along with a decrease in the amount of cover, and it continued to decrease at 250m and the cover also decreased at 250m. An overall inverse relationship between RI leakiness and cover is apparent in Figure 4-1 but this does not show up in the way in which leakiness responds to cover as it changes from 10 to 25m and 25m to 250m resolution..

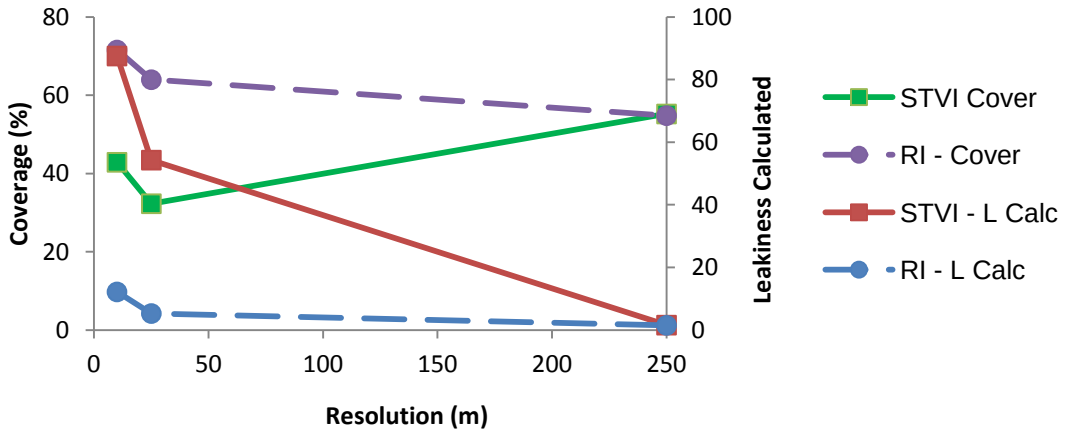

Figure 4-1 Change in cover and leakiness for native scale STVI and RI images

Figure 4-2 shows the pattern of changes that occur when the 10m SPOT image is up-scaled to lower resolutions. STVI cover exhibits a general linear increase while the leakiness calculated from STVI cover values decrease as a negative power of the resolution. A similar pattern of response occurs with RI cover where the amount of cover shows a general linear increase and the RI leakiness decreases as the negative power of the resolution. The general inverse relationship between cover and leakiness is again evident in that the RI cover is higher but the accompanying calculated leakiness is lower..

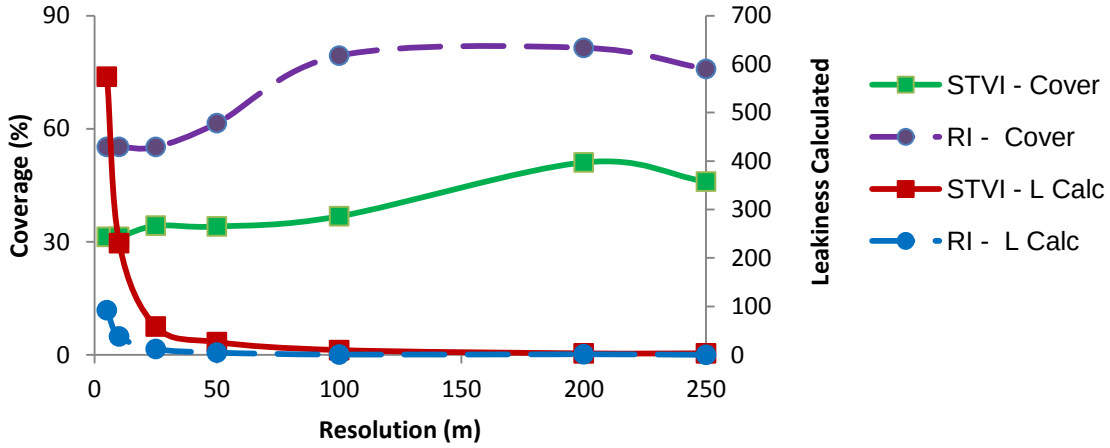

Figure 4-2 Change in cover and leakiness for upscaled STVI and RI images

4.2 Variance

Omnidirectional bounded variograms for the RI and the STVI cover native images at 10, 25 and 250m are shown in Figure 4-3. The 10 and 25m resolution variograms have a spherical structure while the 250m resolution variograms have a nested exponential structure. The Range is between 4-5 pixels at each resolution. The inherent variability based on the sill variance, increases with resolution in the RI images however this partly reverses in the STVI images with the 25m image being less variable than the 10m image. The effect of this variance reversal between RI and STVI images is particularly evident when the semivariance values are plotted as surface contours of resolution and lag as shown in Figure 4-4.

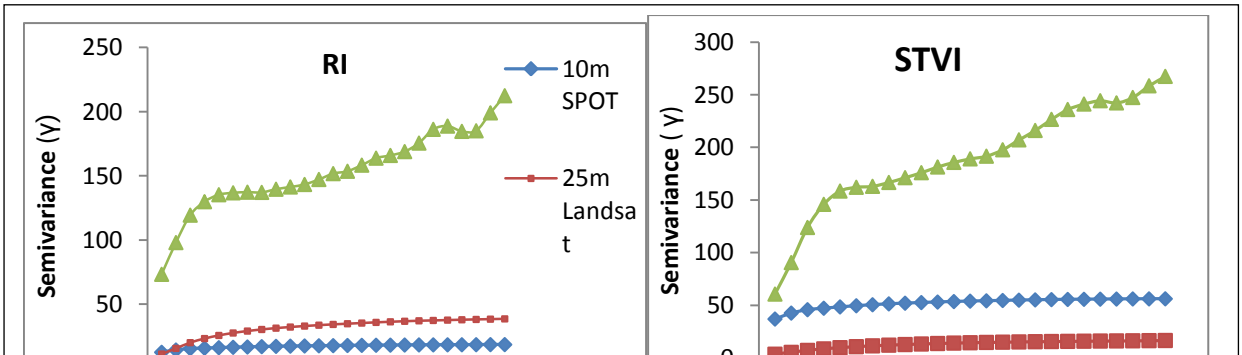

Figure 4-3 Variograms of native resolution coverage grey scale RI and STVI images

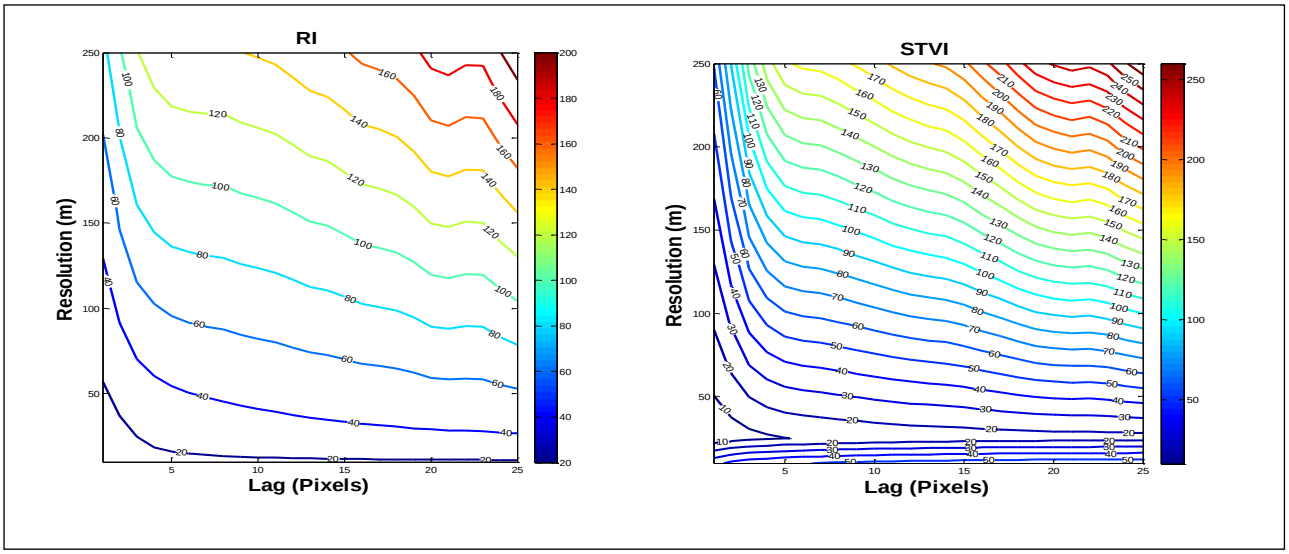

Figure 4-4 Contours of semivariance for native RI and STVI grey scale images

Omnidirectional variograms for the RI and STVI images that have been up-scaled from 5 to 250m are shown in Figure 4-5. These show a different variance pattern when compared to the native image variograms in Figure 4-3. There is a general increase in semi-variance with decrease in resolution (both RI and STVI) however the initial spherical structure evident in the 5m variogram for each type of cover quickly decays into nugget model variograms without defined sills and ranges. This indicates decay of variance with regularization of the image. This decay of variance is further shown in surface contour plots of the variance as a function of the resolution and lag shown in Figure 4-6. The reason for the erratic behavior of the 120γ semi-variance contour is not known.

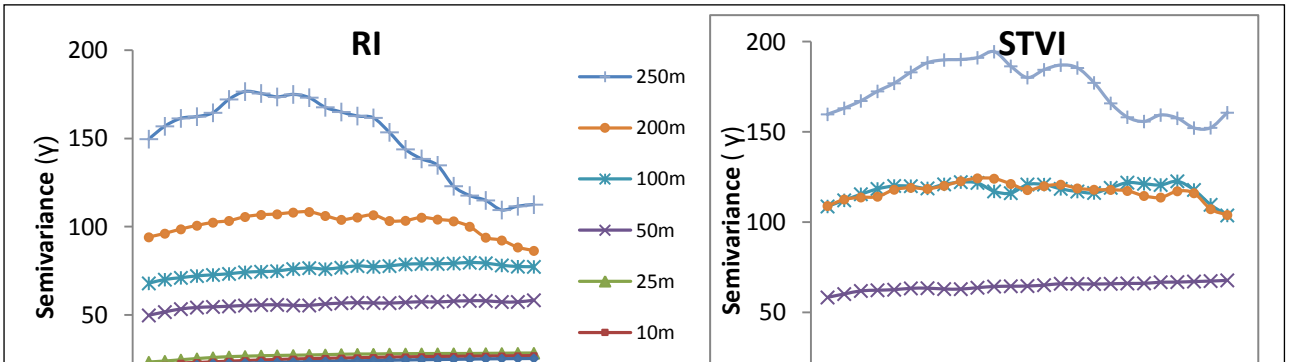

Figure 4-5 Variograms of up-scaled coverage grey scale RI and STVI images

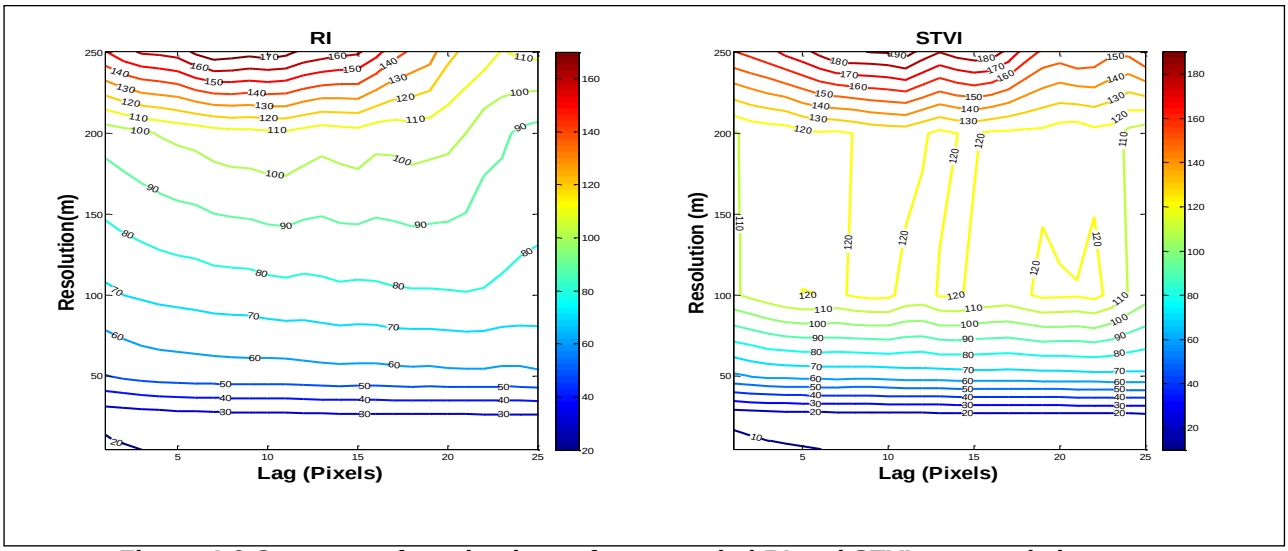

Figure 4-6 Contours of semivariance for up-scaled RI and STVI grey scale images

Indices of variance were extracted from the semivariograms and tested for correlation with the L Calc and Coverage values from the Leakiness analyses for both native scale and up-scaled images. Selected correlation results are shown in Tables 4-1 and 4-2 for RI and STVI images respectively. In most cases the native scale image's values correlate more strongly than the up-scaled image values. This is particularly true for L Calc values.

Table 4-1 Correlation (R^2) of variogram indices and Leakiness variables for RI cover images

	Resolution		First Range		Sill semi-var		Avg Cover		L Calc	
	Native scale	Up-scaled	Native scale	Up-scaled	Native scale	Up-scaled	Native scale	Up-scaled	Native scale	Up-scaled
Resolution	1	1								
First Range	1.000	0.890	1	1						
Sill semi-var	1.000	0.956	1.000	0.740	1	1				
Avg Cover	0.756	0.728	0.756	0.803	0.823	0.641	1	1		
L Calc	0.695	0.356	0.695	0.353	0.680	0.340	0.205	0.399	1	1

Table 4-2 Correlation (R^2) of variogram indices and Leakiness variables for STVI cover images

	Resolution		First Range		Sill semi-var		Avg Cover		Lcalc	
	Native scale	Up-scaled	Native scale	Up-scaled	Native scale	Up-scaled	Native scale	Up-scaled	Native scale	Up-scaled
Resolution	1	1								
First Range	1.000	0.725	1	1						
Sill SV	0.909	0.878	0.909	0.798	1	1				
Avg cover	0.749	0.872	0.749	0.386	0.953	0.609	1	1		
Lcalc	0.735	0.340	0.735	0.200	0.946	0.384	1.000	0.316	1	1

These correlations guided exploration of the following relationships between leakiness variables and changes caused by up-scaling. Figure 4-7 shows that average cover varies widely between native and up-scaled images and between RI and STVI coverage. No indication of a simple relationship is apparent. Figure 4-8 shows that while native scale L Calc values behave differently between RI and STVI changes in average cover, there is a similar negative power response of L Calc to up-scale cover change in both RI and STVI.

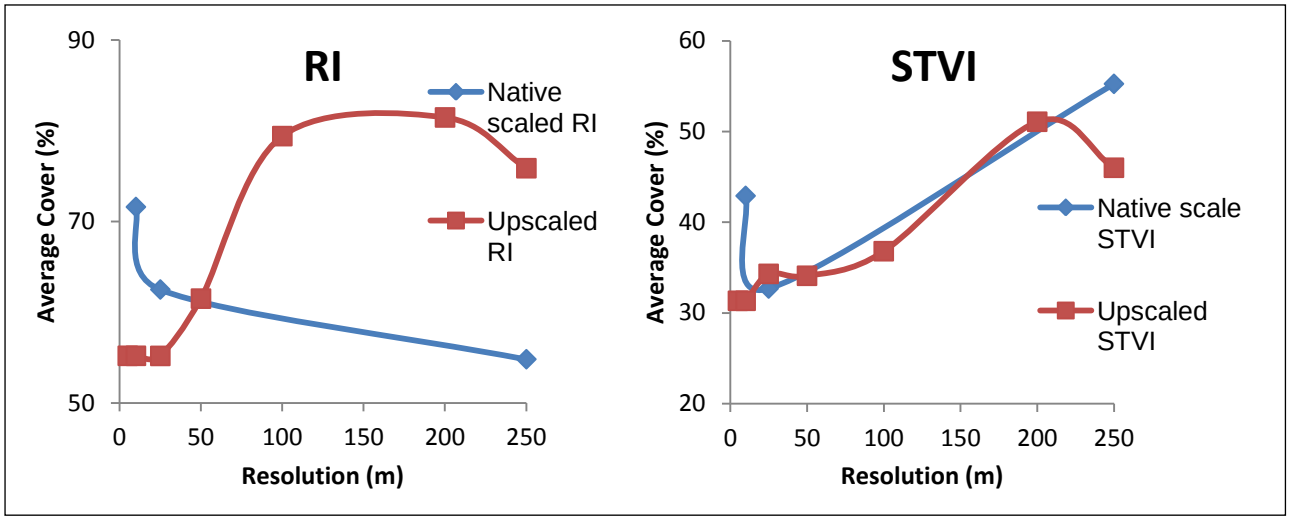

Figure 4-7 Change in RI and STVI cover with change in resolution for native and upscaled images

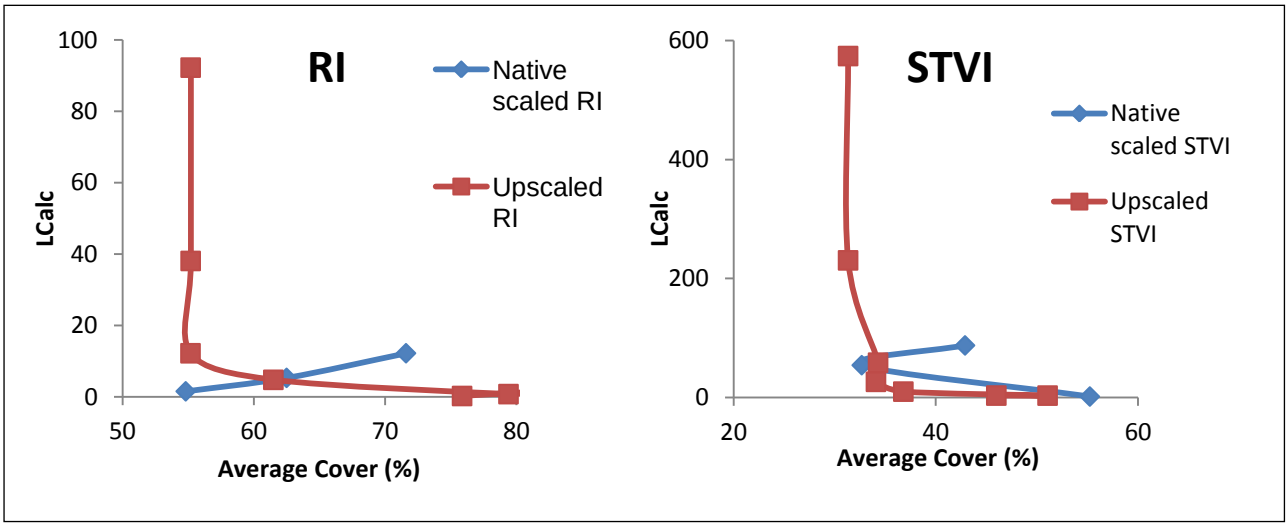

Figure 4-8 Change in L Calc with change RI and STVI cover for native and upscaled images

The nature of the negative power relationship between L Calc and resolution for the up-scaled RI and STVI images is shown in Figure 4-9 with similar power values of -1.411 and -1.36 respectively. A similar type of relationship is also evident for the native scale images.

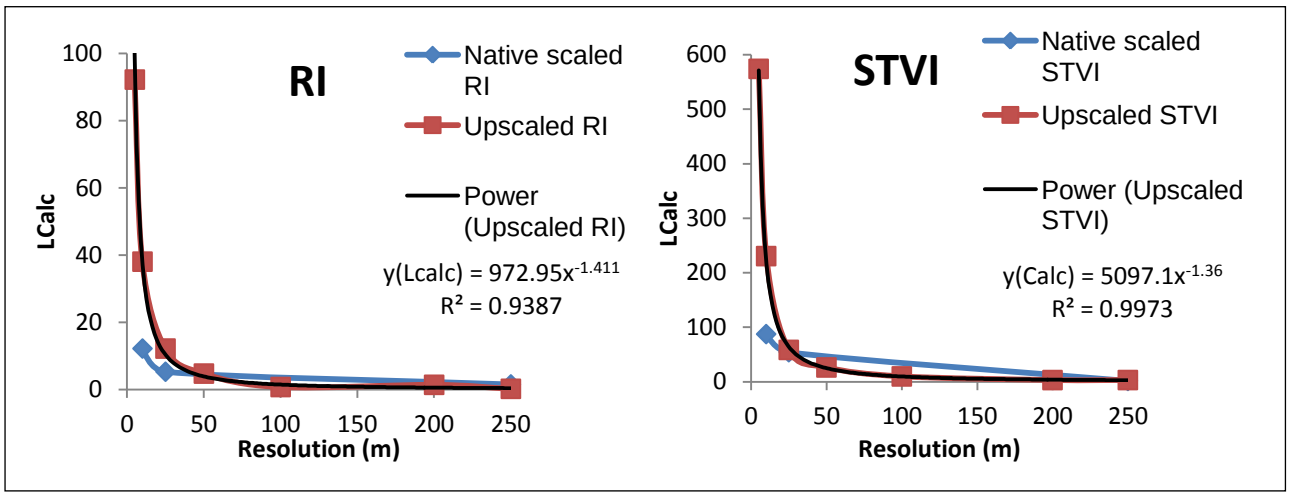

Figure 4-9 Change in L Calc with change in resolution for RI and STVI cover images for native and upscaled images

The indeterminate effect of change in resolution on the sill semivariance for RI and STVI native scaled and up-scaled images is shown in Figure 4-10. Both RI and STVI have a higher smi-variance at the sill at lower resolutions.

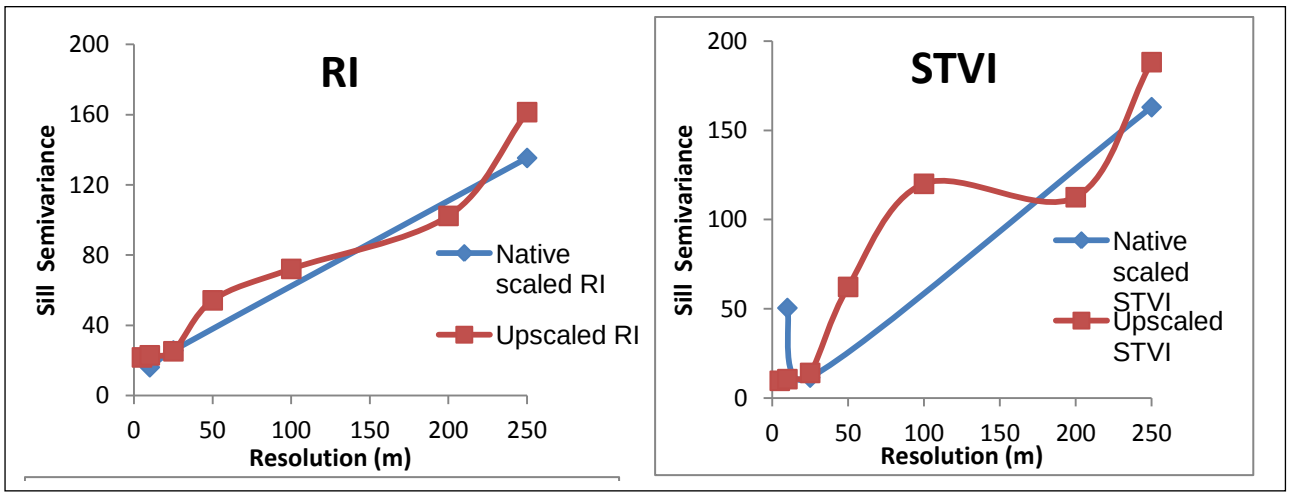

Figure 4-10 Change in sill semivariance for RI and STVI images with change in resolution.

Figure 4-11 shows the negative power relationship between L Calc and the semi-variance at the sill for both RI and STVI up-scaled images. RI also shows a similar relationship for the native scaled images but the STVI native scale relationship is different.

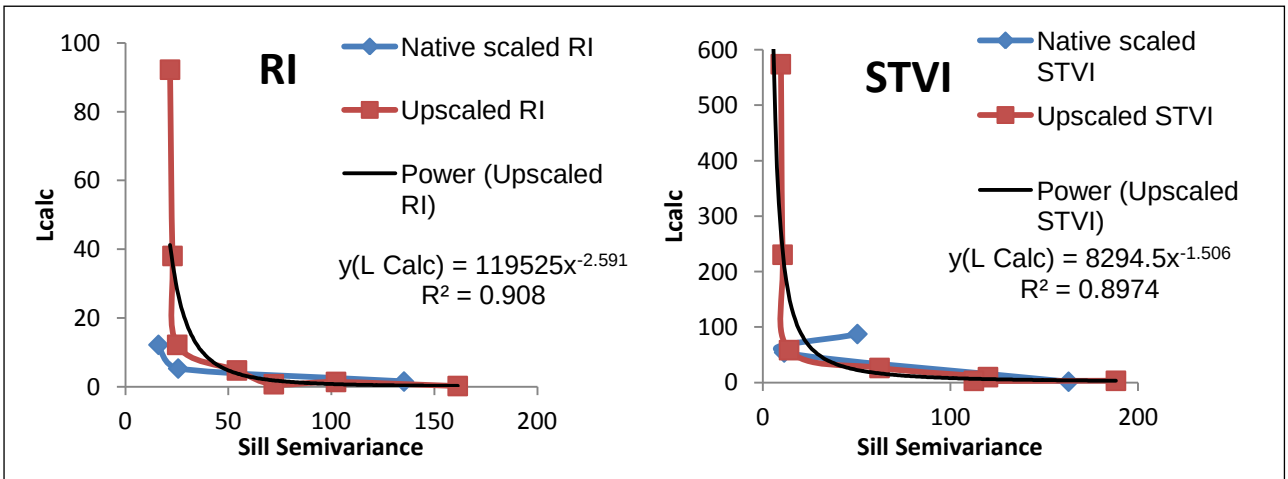

Figure 4-11 Change in L Calc with sill semivariance for RI and STVI for native and upscaled images

5 DISCUSSION

It was expected that the different cover indices would yield different levels of cover because of their different formulae and that the amount of cover might be different in the different concurrent images. This is confirmed in Figure 4-1. However, the increase in STVI cover from 25m to 250m contrasts strongly with the decrease in RI cover between these same resolutions. The joint decrease in STVI cover and leakiness from 10m to 25m is also surprising because a decrease in cover would normally be expected to be accompanied by an increase in leakiness unless there was a marked shift in the location of the cover relative to the catchment pour point accompanying the change in resolution. The decrease in STVI leakiness at 250m is consistent with the increase in STVI cover at this resolution.

The decrease in leakiness accompanying the decrease in RI cover from 10m to 25m change in resolution, while similar to the STVI cover and leakiness at these resolutions was also unexpected for the reasons given previously. Likewise the further decline in RI leakiness accompanying the decline in RI cover at 250m resolution was unexpected (Fig 4-1).

When the 10m SPOT image was upscaled the STVI and RI cover values increased in a generally linear manner as shown in Figure 4-2. The plateau between 100 and 200m resolution followed by a decline at 250m for RI cover is unexplained. The upscaled values at 25m and 250m (Fig. 4-2) did not approach the native scale values for 25m and 250m (see Fig. 4-1). Catchment leakiness for both upscaled STVI and RI images decreased as a negative power of the resolution.

Both the advent of imagery of widely different resolutions and the need to perform assessments of large areas has led to the common practice of image aggregation by resampling. Collins et al., (1999) wisely cautioned that "*creating coarse-resolution data by averaging blocks of fine-resolution pixels is, at best, a rough approximation of the way in which remote sensing devices operate*". This is due in large part to the failure of aggregating processes to reflect the Point Spread Function of the sensor that leads to the generation of the pixel DN values. Despite this caution, and also because of it, the cubic convolution method of aggregation (ESRI 2012) was considered the best available method for upscaling the 10m SPOT imagery.

Differences in the statistical behavior between native scale and upscaled images were analysed using variograms. The change in variance between the 10, 25 and 250m native scale images is shown in Figures 4-3 and 4-4. The 10 and 25m native image variograms are spherical (Collins et al., 1999) while the 250m variograms are exponential with evidence of structural nesting. These changes are likely to be due to different scales measuring the semivariance of different landscape features. This raises the question as to what the features are at each resolution level and whether or not they are features that influence leakiness.

Higher resolution features may be expected to have lower nuggets and sill semivariances (Collins et al., 1999). This occurs with the RI 10 and 25m images when compared to the 250m image. The reason the STVI 10m image has a higher nugget and sill semivariance than the 25m image is unexplained. Both RI and STVI native scale images show a regular pattern of semi-variance contours at higher resolutions (low pixel dimension) with evidence of feature nesting at lower resolutions at high lags (Figure 4-4).The upscaled image variograms (Figure 4-5) and semivariance contours (Figure 4-6) show a progressive decay in the internal variance structure of the image as it is upscaled.

Many measurement indices can be derived from variograms and these can assist with classifying landscape structures (Balaguer et al., 2010). The first range and sill semivariance indices were analysed for correlation with image resolution, average cover and leakiness. The results for native and upscaled RI and STVI grey scale images are shown in Tables 4-1 and 4-2.

These were used to identify possible explanatory relationships between the image and leakiness variables. The reason the native scale image variance indices correlate more strongly than the upscaled image variances (one exception, Table 4-1) with both coverage and leakiness of the imagery is thought to be due to the known effect of regularisation on degrading image variance (Turner et al., 1989; Wu 2004).

The amount of average cover of concurrent images at different resolutions of the same area is different (Figure 4-7). The potential reasons for this, range from the small difference in capture date for the Landsat image (one month after the SPOT and MODIS images) to sensor spectral differences and spatial feature recognition differences. The behavior of upscale average cover values was unpredictable.

Leakiness increased linearly with increase in native scale RI cover but the relationship with STVI cover was inverted. When upscaled, leakiness had a negative power relationship with both RI and STVI cover (Figure 4-8). Leakiness also had a negative power relationship with resolution for RI and STVI native and upscaled images (Figure 4-9).

Sill semivariance did not change with resolution in any easily explained way as shown in Figure 4-10. However, the leakiness of upscaled images correlated well (RI, R^2=0.908 and STVI, R^2=0.8974) with sill semivariance (Figure 4-11). This also held for native scale RI leakiness values but not for STVI leakiness.

The uncertainties created by these results serve to caution the use of the Leakiness Calculator for catchment leakiness assessment with respect to comparison of results between different types of images taken at different resolutions and at different times. Any preprocessing steps that incorporate regularisation should also be carefully considered. Potential causes of variation need to be controlled in the design of any assessment in which results from one area are to be compared with the results from another area.

6 CONCLUSION

This study investigate the effect of scale on landscape function analysis through use of the CSIRO Leakiness Calculator and two cover indices applied to a grazing catchment in the dry tropics area of North Queensland. The two different cover indices produced different cover and leakiness results at any given image scale. Cubic convolution resampling was used to upscale the high resolution images to match the lower resolution images. The upscaled images produced different cover and leakiness results from the native scale images of the same scale.

The reasons underlying the differences in results were investigated using semivariance techniques. Preliminary conclusions are that leakiness cannot be reliably calculated from resampled imagery because the Leakiness Calculator model relies on both the identification of the flow restricting landscape features and their location in the catchment flow path. Upscale resampling degrades the landscape features as evidenced by the decay in the structure of the variograms. This is accompanied by higher nugget values indicative of increased noise variance and a lower sill variance indicating decay of landscape feature variance.

These results also raise questions about the failure of coincident imagery from different sensors to yield comparable leakiness results, the different leakiness responses to similar amounts of cover of different types and the suitability of different land cover indices to represent landscape feature flow restrictions. This raises the following questions; i. what scale of imagery should be used to get reliable results from the Leakiness Calculator, ii. Does this scale vary with the type of landscape, and iii. What features of the landscape determine the ideal image scale?

7 ACKNOWLEDGEMENTS

The authors wish to acknowledge the generous assistance from the Queensland Department of Environment and Resource Management, in particular the assistance of Dr. Peter Scarth, Ms. Jasmine Muir, Mr. Adrian Neal and Mr. Mehedi Etemadi, the cooperation and assistance of the graziers who gave generously and selflessly of their time during our ground truth studies, Mr. David Tongway, Dr. Adam Liedloff, Mr. John Ludwig and Dr. Brett Abbott of CSIRO for their assistance, supply of data and consultation, Mr. Robert Karfs of the Queensland Department of Primary

Industries for his practical advice and Mr. Doug Willis of the Queensland Northern Dry Tropics NRM Body and Mr. Lee Blacklock of the NRM Regional Cooperatives Group for their generous assistance in supplying satellite imagery. Finally, consultation with the above people would not have been possible without the assistance of NCCARF travel grant number

.

8 REFERENCES

[1] Atkinson, P. M. (2004). Resolution Manipulation and Sub-Pixel Mapping. Remote Sensing Image Analysis: Including the Spatial Domain. S. M. de Jong and F. D. van der Meer. London, Kluwer.

[2] Atkinson, P. M. and N. J. Tate (2000). "Spatial Scale Problems and Geostatical Solutions: A Review." Professional Geographer **52**(4): 607.

[3] Balaguer, A., L. A. Ruiz, et al. (2010). "Definition of a comprehensive set of texture semivariogram features and their evaluation for object-oriented image classification." Computers & Geosciences **36**(2): 231-240.

[4] Bannari, A., D. Morin, et al. (1995). "A review of vegetation indices." Remote Sensing Reviews **13**(1-2): 95-120.

[5] Bastin, G., B. Abbott, et al. (2008). Validating a remotely sensed index of Landscape Leakiness in the Burdekin Dry Tropics. Water for a Healthy Country National Research Flagship. Queensland, CSIRO.

[6] Bastin, G., J. A. Ludwig, et al. (2002). "Indicators of landscape function: comparing patchiness metrics using remotely-sensed data from rangelands." Ecological Indicators **1**(4): 247-260.

[7] Bastin, G., P. Scarth, et al. (2012). "Separating grazing and rainfall effects at regional scale using remote sensing imagery: A dynamic reference-cover method." Remote Sensing of Environment **121**: 443-457.

[8] Bian, L. and R. Butler (1999). "Comparing effects of aggregation methods on statistical and spatial properties of simulated spatial data." Photogrammetric Engineering and Remote Sensing **65**(1): 73-84.

[9] Bradshaw, G. A. and M. J. Fortin (2000). "Landscape Heterogeneity Effects on Scaling and Monitoring Large Areas Using Remote Sensing Data." Annals of GIS **6**(1): 61-68.

[10] Collins, J. B. and C. E. Woodcock (1999). "Geostatistical estimation of resolution dependent variance in remotely sensed images." Photogrammetric Engineering and Remote Sensing **65**(1): 41-50.

[11] Corfield, J. P., B. N. Abbott, et al. (2006). PATCHKEY: a patch classification frameworkfor the upper Burdekin and beyond. Proceedings of the Australian Rangeland Conference.

[12] CSIRO (2007). CSIRO Leakiness Calculator: Basic instructions for use. Darwin, Australia, CSIRO, Sustainable Ecosystems Section.

[13] De Jong, S. M., R. Pebesma, et al. (2011). Spatial variability, Mapping Methods, Image Analysis and Pixels. Remote Sensing Image Analysis: Including the Spatial Domain. S. M. d. J. a. F. D. V. d. Meer. New Delhi, Kluwer Academic Publishers**:** 17-36.

[14] ESRI. (2012). "Arc GIS Resource Center." Retrieved 5 Dec 2012, 2012, from http://help.arcgis.com/en/arcgisdesktop/10.0/help/index.html#//00590000001m000000.

[15] Garrigues, S., D. Allard, et al. (2008). "Multivariate quantification of landscape spatial hetereogeneity using variogram models." Remote Sensing of Environment **112**: 216-230.

[16] Jafari, R., M. M. Lewis, et al. (2007). "Evaluation of vegetation indices for assessing vegetation cover in southern arid lands in South Australia." The Rangeland Journal **29**(1): 39-49.

[17] Karl, J. W. and B. A. Maurer (2010). "Spatial dependence of predictions from image segmentation: A variogram-based method to determine appropriaqte scales for producing land management information." Ecological Informatics **5**: 194-202.

[18] Ludwig, J., G. N. Bastin, et al. (2007a). "Leakiness: A new index for monitoring the health of arid and semiarid landscapes using remotely sensed vegetation cover and elevation data." Ecological Indicators **7**(2): 442-454.

[19] Ludwig, J., R. Eager, et al. (2002). "A leakiness index for assessing landscape function using remote sensing." Landscape Ecology **17**(2): 157-171.

[20] Ludwig, J., R. W. Eager, et al. (2006). "A new landscape leakiness index based on remotely sensed ground-cover data." Ecological Indicators **6**(2): 327-336.

[21] Ludwig, J. and D. Tongway (1997). A Landscape Approach to Rangeland Ecology, in 'Landscape Ecology, Function and management: Principles from Australia's Rangelands' (Eds J. Ludwig, D. Tongway, D Freudenberger, J.C. Noble and K. Hodgkinson). Melbourne, CSIRO.

[22] Ludwig, J., D. J. Tongway, et al. (2004). "Monitoring ecological indicators of rangeland functional integrity and their relation to biodiversity at local to regional scales." Austral Ecology **29**(1): 108-120.

[23] Ludwig, J., J. A. Wiens, et al. (2000). "A Scaling Rule for Landscape Patches and How it Applies to Conserving Soil Resources in Savannas." Ecosystems **3**: 84-97.

[24] Ludwig, J. A., R. Bartley, et al. (2007b). "Patch configuration non-linearly affects sediment loss across scales in a grazed catchment in north-east Australia." Ecosystems **10**(5): 839-845.

[25] Ostendorf, B. and J. F. Reynolds (1993). "Relationships between a terrain based hydrologic model and patch scale vegetation patterns in an arctic tundra landscape." Landscape Ecology **8**(4): 229-237.

[26] Pickup, G., G. N. Bastin, et al. (2000). "Measuring rangeland vegetation with high resolution airborne videography in the blue-near infrared spectrum region." International Journal of Remote Sensing **21**(2): 339-351.

[27] Pickup, G., V. H. Chewings, et al. (1993). "Estimating changes in vegetation cover over time in arid rangelands using landsat MSS data." Remote Sensing of Environment **43**(3): 243-263.

[28] Ruiz, L. A., J. A. Recio, et al. (2011). "A feature extraction software tool for agricultural object-based image analysis." Computers and Electronics in Agriculture **76**(2): 284-296.

[29] Scarth, P. F., M. Byrne, et al. (2006). State of the Paddock: monitoring condition and trend ground cover across Queensland. Q. D. o. E. a. R. Management. Brisbane.

[30] Scarth, P. F., M. Byrne, et al. (2008). State of the Paddock: monitoring condition and trend ground cover across Queensland. Q. D. o. E. a. R. Management. Brisbane.

[31] Schmidt, M., R. J. Denham, et al. (in prep). "Large scale fractional ground cover monitoring based on long term field observations and Landsat satellite imagery.".

[32] Thenkabail, P. S., A. D. Ward, et al. (1994). "Thematic mapper vegetation indices for determining soybean and corn growth parameters." Photogrammetric Engineering and Remote Sensing **60**: 437-442.

[33] Tongway, D. and N. Hindley (2004). "Landscape function analysis: a system for monitoring rangeland function." African Journal of Range & Forage Science **21**(2): 109-113.

[34] Tongway, D. and J. A. Ludwig (1990). "Vegetation and soil patterning in semi-arid mulga lands of Eastern Australia." Australian Journal of Ecology **15**: 23-34.

[35] Turner, M. G., R. V. O'Neill, et al. (1989). "Effects of changing spatial scale on the analysis of landscape pattern." Landscape Ecology **3**(3): 153-162.

[36] Wilcox, B. P., D. D. Breshears, et al. (2003). "Ecohydrology of a resource- conserving semiarid woodland: Effects of scaling and disturbance." Ecological Monographs **73**: 223-239.

[37] Wu, J. (2004). "Effects of changing scale on landscape pattern analysis: scaling relations." Landscape Ecology **19**(2): 125-138.

[38] Wu, J., W. Shen, et al. (2002). "Empirical patterns of the effects of changing scale on landscape metrics." Landscaape Ecology **17**: 761-782.